

Heterozygous *UCHL1* loss-of-function variants cause a neurodegenerative disorder with spasticity, ataxia, neuropathy, and optic atrophy

Joohyun Park,^{1,36} Arianna Tucci,^{2,36} Valentina Cipriani,^{2,3,4,5,36} German Demidov,¹ Clarissa Rocca⁶, Jan Senderek,⁷ Michaela Butyrn,⁸ Ana Velic,⁹ Tanya Lam,^{10,11} Evangelia Galanaki,¹² Elisa Cali,¹² Letizia Vestito,² Reza Maroofian,¹² Natalie Deininger,¹ Maren Rautenberg,¹ Jakob Admard,¹ Gesa-Astrid Hahn,¹³ Claudius Bartels,¹⁴ Nieke van Os,¹⁵ Rita Horvath,¹⁶ Patrick Chinnery,¹⁷ May Tiet,¹⁸ Channa Hewanmadduma,^{19,20} Marios Hadjivassiliou,^{20,21} George K. Tofaris,²² Genomics England Research Consortium, Nicholas W. Wood,²³ Stefanie Hayer,^{24,25} Friedemann Bender,^{24,25} Benita Menden,¹ Isabell Cordts,^{1,26} Joachim K. Krauss,²⁷ Christian Blahak,^{28,98} Tim M. Strom,^{30,31} Marc Sturm,¹ Bart van de Warrenburg,¹⁵ Holger Lerche,³² Boris Maček,⁹ Matthis Synofzik,^{23,24} Stephan Ossowski,¹ Dagmar Timmann,³³ Marc Wolf,^{28,34} Damian Smedley,² Olaf Riess,^{1,35} Ludger Schöls,^{24,25,35*} Henry Houlden,^{2,37**} Tobias B. Haack,^{1,34,76} Holger Hengel,^{1,24,25,37}

¹Institute of Medical Genetics and Applied Genomics, University of Tübingen, 72076 Tübingen, Germany

²William Harvey Research Institute, School of Medicine and Dentistry, Queen Mary University of London, London EC1M 6BQ, UK

³UCL Institute of Ophthalmology, University College London, London EC1V 9EL, UK

⁴Moorfields Eye Hospital NHS Foundation Trust, London EC1V 2PD, UK

⁵UCL Genetics Institute, University College London, London WC1E 6AA, UK

26 ⁶Department of Neuromuscular Diseases, University College London Queen Square Institute
27 of Neurology, London WC1N 3BG, UK

28 ⁷Friedrich-Baur-Institute at the Department of Neurology, University Hospital, LMU Munich,
29 80336 Munich, Germany

30 ⁸German Center for Neurodegenerative Diseases (DZNE), 39120 Magdeburg, Germany

31 ⁹Proteome Center Tübingen, University of Tübingen, 72076 Tübingen, Germany

32 ¹⁰Great Ormond Street Hospital NHS Trust, London WC1N 3JH, UK

33 ¹¹St George's Hospital NHS Trust, London SW17 0QT, UK

34 ¹²Department of Neuromuscular Diseases, University College London Queen Square
35 Institute of Neurology, London WC1N 3BG, UK

36 ¹³CeGaT GmbH, Center for Genomics and Transcriptomics, 72076 Tübingen, Germany

37 ¹⁴Department of Neurology, Otto-von-Guericke University, 39120 Magdeburg, Germany

38 ¹⁵Department of Neurology, Donders Institute for Brain, Cognition and Behavior, Center of
39 Expertise for Parkinson and Movement Disorders, Radboud University Medical Center, 6525
40 GA Nijmegen, The Netherlands.

41 ¹⁶Department of Clinical Neurosciences, University of Cambridge, John Van Geest
42 Cambridge Centre for Brain Repair, Cambridge Biomedical Campus, Cambridge CB2 0PY,
43 UK

44 ¹⁷MRC Mitochondrial Biology Unit & Department of Clinical Neurosciences, University of
45 Cambridge, Cambridge Biomedical Campus, Cambridge CB2 0QQ, UK

46 ¹⁸Department of Clinical Neurosciences, University of Cambridge, Cambridge CB2 0QQ, UK

47 ¹⁹Sheffield Institute for translational neurosciences (SITRAN), University of Sheffield,
48 Sheffield S10 2HQ UK

49 ²⁰Royal Hallamshire Hospital, Sheffield Teaching Hospitals Foundation Trust , Sheffield S10
50 2JF, UK

51 ²¹Academic Department of Neurosciences, Sheffield Teaching Hospitals NHS Trust and
52 University of Sheffield, Sheffield S10 2JF, UK

53 ²²Nuffield Department of Clinical Neurosciences, University of Oxford, Oxford, UK

²³Department of Clinical and Movement Neurosciences, University College London Queen
Square Institute of Neurology, London, UK.

²⁴Department of Neurology and Hertie-Institute for Clinical Brain Research, University of
Tübingen, 72076 Tübingen, Germany

²⁵German Center of Neurodegenerative Diseases (DZNE), 72076 Tübingen, Germany

²⁶Department of Neurology, Klinikum rechts der Isar, Technical University Munich, Munich,
Germany

²⁷Department of Neurosurgery, Hannover Medical School, 30625 Hannover, Germany

²⁸Department of Neurology, Ortenau Klinikum Lahr-Ettenheim, 77933 Lahr, Germany.

²⁹Department of Neurology, Universitätsmedizin Mannheim, Medical Faculty Mannheim,
University of Heidelberg, 68167 Mannheim, Germany

³⁰Institute of Human Genetics, Technische Universität München, 81675 Munich, Germany

³¹Institute of Human Genetics, Helmholtz Zentrum München, 85764 Neuherberg, Germany

³²Department of Neurology and Epileptology, Hertie Institute for Clinical Brain Research,
University of Tübingen, 72076 Tübingen, Germany

³³Department of Neurology, Essen University Hospital, University of Duisburg-Essen, 45147
Essen, Germany

³⁴Department of Neurology, Klinikum Stuttgart, 70174 Stuttgart, Germany

³⁵Center for Rare Diseases, University of Tübingen, 72076 Tübingen, Germany

³⁶These authors contributed equally to this work

³⁷These authors contributed equally to this work

Correspondence to:

*Ludger Schöls, MD, Department of Neurology and Hertie-Institute for Clinical Brain Research,
University of Tübingen, Otfried-Müller-Straße 27, 72076 Tübingen, Germany. E-mail:
ludger.schoels@uni-tuebingen.de

81 **Henry Houlden, MD, PhD, Department of Neuromuscular Disorders, Institute of Neurology,
82 University College London, Queen Square, WC1N 3BG London, UK. E-mail:
83 h.houlden@ucl.ac.uk

ABSTRACT (154/250 words)

Bi-allelic missense and putative splice variants in *UCHL1* (*Ubiquitin C-terminal hydrolase L1*) have been associated with severe early-onset, autosomal recessive spastic paraplegia type 79, which is characterized by progressive visual loss, ataxia, and spasticity. By case-control burden analysis in independent cohorts of hereditary spastic paraplegia and ataxia patients from Germany and the U.K., we prioritized *UCHL1* as a candidate gene for an autosomal dominant disorder. We identified a total of 33 cases from 17 unrelated families, providing evidence that loss-of-function variants in *UCHL1* cause an autosomal dominant neurodegenerative disorder characterized by spasticity, ataxia, neuropathy and/or optic atrophy. Disease onset varied between childhood and 70 years of age with the majority of individuals showing a late-onset (median 49) and mild progression of disease. Using patients' fibroblasts, we confirmed an approximately 50% reduction of *UCHL1* in mass spectrometry-based proteomics. Through transcriptomic data we explored dysregulated pathways and showed a possible involvement of *UCHL1* in amyloid degradation pathways.

Keywords: *UCHL1*, spastic ataxia, transcriptomics, proteomics, amyloid degradation

INTRODUCTION

Hereditary ataxias (HAs) and hereditary spastic paraplegias (HSPs) are both rare neurogenetic diseases, affecting mainly the cerebellar and pyramidal system, respectively. Clinical overlap between these rare diseases is frequently observed¹⁻³. Besides the clinical overlaps, advances in next-generation sequencing have shown that there is also a shared genetic basis and molecular pathophysiology of these disorders suggesting a shared vulnerability of cerebellar and corticospinal neurons. At least 69 genes with autosomal dominant, autosomal recessive or X-linked inheritance have been described to cause disorders on a phenotypic spectrum overlapping HSPs and HAs⁴. Application of exome (ES) and genome sequencing (GS) in routine diagnostic setting drastically increased the diagnostic yield and the extent of generated genetic data. Yet it is estimated that ES leads to a genetic diagnosis only in half of the affected individuals with HSPs and/or HAs⁵. Analytic strategies in routine diagnostic settings are mostly single family/individual-based and do not usually involve large cohorts for the identification of rare disease causal genetic variation. Data sharing and increasing availability of large rare disease cohorts open the perspective to realize the potential of cohort-based burden analyses even for these rare disorders. Here, we used case-control gene-burden analysis in independent cohorts of patients with HSPs and HAs, and discovered *ubiquitin C-terminal hydrolase L1 (UCHL1)* as a gene for an autosomal dominant neurodegenerative disorder.

UCHL1 has previously been associated with autosomal recessive spastic paraplegia type 79 (SPG79), characterized by early-onset cerebellar ataxia, spastic paraplegia, and optic atrophy.⁶⁻⁸ It encodes a deubiquitinating enzyme, that is neuron-specific and one of the most abundantly expressed proteins in the brain, constituting approximately 1 to 2% of soluble protein.^{9, 10} It is essential for maintaining ubiquitin homeostasis and its absence leads to aggregation of ubiquitinated proteins which is a common hallmark for many neurodegenerative diseases.^{11, 12} The role of *UCHL1* variants in numerous neurodegenerative disorders such as Alzheimer's disease (AD), Parkinson's disease (PD) and amyotrophic lateral sclerosis (ALS),

have been widely explored, but the exact impact of *UCHL1* on the pathogenesis of these diseases could not be clarified so far.¹³⁻¹⁵

By applying burden analyses, we report 33 probands with predicted loss-of-function variants (LoFs) in *UCHL1*, and establish *UCHL1* to be associated with an autosomal dominant neurodegenerative disorder characterized by late-onset spastic-ataxia, neuropathy, and often optic atrophy. Combined analyses of untargeted transcriptomic and proteomic datasets from patients' fibroblasts suggested haploinsufficiency as the likely disease mechanism and a possible role of *UCHL1* in protein degradation pathways.

MATERIALS, SUBJECTS AND METHODS

Ethical approval

German cohort: written informed consent was obtained from all individuals or their guardians. The study was approved by the ethics committee of the medical faculty by the local Institutional Review Board of the Medical Faculty of the University of Tübingen, Germany (vote 598/2011 and BO1066/2021BO2).

U.K. cohort within the 100,000 Genomes Project (100KGP): following ethical approval from the the national research ethics committee (14/EE/1112), consent was obtained from all patients recruited to the 100KGP.¹⁶

Genetic investigation

German cohort: diagnostic ES and GS were conducted in routine clinical care at the Institute of Medical Genetics and Applied Genomics Tübingen (Tübingen, Germany) as described previously.^{17, 18} Exome and genome sequencing libraries were generated from genomic DNA using Agilent SureSelect XT Human All Exon V5/V7 enrichment kits (Agilent Technologies, Santa Clara, CA, USA) or the TruSeq DNA PCR-Free k5it (Illumina, San Diego, CA, USA), respectively. Sequencing was performed on a HiSeq2500 [2 x 125, 2 x 100 base pairs (exome); Illumina, San Diego, CA, USA] or NovaSeq 6000 system [2 x 150 base pairs

(genome); Illumina, San Diego, CA, USA] as paired-end reads. The sequence data was analyzed using the megSAP pipeline (<https://github.com/imgag/megSAP>) and aligned to the GRCh37 reference genome. Copy-number variations (CNVs) were analyzed using an in-house developed CNV calling tool. Prior to burden analysis all datasets have been analyzed in a diagnostic setting according to an in-house standard operating procedure including a variety of different filtering steps to prioritize likely clinically relevant DNA variants. Identified variants were classified following the recommendations of the American College of Medical Genetics and Genomics.¹⁹

U.K. cohort within the 100KGP: DNA extracted from blood was prepared for GS using TruSeq DNA PCR-Free library preparation. 150 or 125 bp paired-end sequencing was performed on either HiSeq 2000 or HiSeq X platforms. Genomes were sequenced to an average minimum depth of 35X (31X - 37X); sequencing reads were aligned to the human genome reference build 37 or build 38 using of Isaac Genome Alignment Software. Family-based variant calling of single-nucleotide variants (SNVs) and insertion or deletions (indels) was performed with the use of the Platypus variant caller.

Gene burden analysis

German cohort: case-control gene burden analysis was performed on 1,547 selected diagnostic cases from the in-house database at the Institute of Medical Genetics and Applied Genomics Tübingen presenting with either spastic paraplegia, ataxia, or spastic ataxia and 3,624 controls (i.e. healthy controls, patients with non-related diseases) using burden test implemented in rvGWAS package.²⁰ Related family members were excluded from both groups. Population was defined using megSAP pipeline and only European descent samples were used for cases and controls. Male and female ratio was matched between the case and control cohorts. Non-synonymous variants, including splice site alterations (± 20 nucleotides from exon-intron boundary) involving any of the ~ 20,000 consensus coding sequence (CCDS) genes, were extracted followed by filtering steps to define qualifying variants. Only variants with at least 20x coverage were included. We focused on rare variants with a minor allele

frequency (MAF) of < 0.5% in gnomAD (v2.1.1 and v3.1.1, Genome Aggregation Database, gnomad.broadinstitute.org) and a MAF of < 2.5% in an in-house database. Only variants with high impact (annotated as start-lost, stop-gain, frameshift, and canonical splice site alterations located ± 2 nucleotides) or high pathogenicity scores (CADD score > 25 or SIFT/PolyPhen damaging annotation) were selected. To control the false discovery rate (FDR), the overall p value from the gene burden testing was adjusted using the Benjamini-Hochberg procedure. Subsequently, enrichment of *UCHL1* variants in HSPs and HAs was evaluated in the full in-house dataset of 14,303 exomes and genomes at the Institute of Medical Genetics and Applied Genomics Tübingen. At the time of the study, 2,066 out of 14,303 individuals were reported to show spasticity and/or ataxia. Among them, only 272 were described to present both spastic paraplegia and ataxia. The enrichment of rare variants in cases was analyzed by one-sided Fisher's exact test using R statistical Software (<https://www.r-project.org/>). A p value < 2.5×10^{-6} was used to claim gene-based genome/exome-wide significance corrected for ~20,000 CCDS genes.

U.K. cohort within the 100KGP: case-control gene burden analysis was performed within the rare disease component of the 100KGP.¹⁶ Cases were defined as all 100KGP probands recruited under a certain clinical indication, e.g. 'hereditary ataxia', while corresponding 'controls' were all remaining recruited 100KGP probands except those recruited under the broader disease category of the clinical indication, e.g. 'neurological and neurodevelopmental disorder'. Exomiser was then run on all probands' genome data to filter (i) rare (MAF < 0.1%, for dominant, and <1%, for recessive, in gnomAD v2.1.1 and v3.1.1), (ii) coding variants, (iii) that segregated with the disease status (if multiple family members were available) as expected for each possible mode of inheritance.²¹ Gene-based enrichment of rare variants in cases was assessed using one-sided Fisher's exact tests under four scenarios: (1) enrichment of rare, predicted LoFs, (2) enrichment of rare, predicted pathogenic variants (with Exomiser variant score > 0.8, that is variants that are predicted to be pathogenic by in silico prediction tools REVEL [8] and/or MVP [9]), (3) enrichment of rare variants with Exomiser variant score > 0.8 and in a constrained coding region [10], (4) enrichment of rare, de novo

variants. For the latter, only trios or larger families where de novo calling was possible were considered. The Benjamini and Hochberg method was used to correct for multiple testing; an overall false discovery rate adjusted q value threshold of 0.10 was used for claiming significant gene-disease associations taking into account the total number of test under all four scenarios and all 100KGP clinical indications analysed, i.e., 621,741.

All 100KGP genomes were screened for SNVs, small deletions/ insertions and CNVs and short tandem repeats (STRs) in genes from the PanelApp virtual gene panels for HA and HSP. CNV calls were generated by Genomics England using Manta and Canvas software (Illumina); STR calls were generated using ExpansionHunter.^{22, 23} No likely pathogenic variants were identified.

Clinical investigation

Patients from Germany were examined and phenotyped by experienced neurologists and referred to the genetic center at the University of Tübingen for diagnostic ES or GS. Detailed clinical data of individuals with LoFs in *UCHL1* were obtained and analyzed.

Patients from the U.K. with genetically undiagnosed neurological disease were recruited to the 100KGP by neurologists at English hospitals. At recruitment, standardized clinical data were recorded using the Human Phenotyping Ontology, according to disease-specific data model (<https://www.genomicsengland.co.uk/?wpdmdl=5500>).²⁴ Following the identification of families carrying *UCHL1* LoFs with spastic ataxia by gene burden analysis, additional information was collected retrospectively by contacting the recruiting clinician for each patient (summarized in Table S7).

Fibroblast cultivation and protein isolation

Human dermal fibroblasts were maintained at 37°C, 5% CO₂ and 100% relative humidity in fibroblast medium consisting of Dulbecco's Modified Eagle Medium (Merck) supplemented with 10% foetal bovine serum (Thermo Fisher Scientific) in cell culture flasks. Upon reaching high confluence, primary fibroblasts were washed with cold PBS, scraped off

in PBS, centrifuged at 800 g for 5 min and frozen at -80°C. Pellets of primary fibroblasts were lysed in RIPA buffer (Sigma) containing protease inhibitors (Roche) for 45 min on a rotator at 4°C. Cell debris were pelleted at 15,800 g and 4°C for 30 min. The protein concentration was determined using the Pierce BCA Protein Assay Kit (Thermo Fisher Scientific) according to the manufacturer's instructions.

RNA isolation and RNA sequencing

For RNA extraction, fibroblasts from five primary proband fibroblast cell lines (F1-IV.1, F1-IV.3, F2-III.3, F2-IV.1, F3-II.1) and five primary control fibroblast cell lines (age and gender matched) were cultivated. RNA was isolated from two independently grown flasks for each cell line (biological replicates, 10x2 RNA samples) using the QIAGEN RNeasy Mini Kit. RNA quality was assessed with the Agilent 2100 Bioanalyzer RNA Nano Kit (Agilent Technologies, Inc., Santa Clara, United States). All samples had high RNA integrity numbers (RIN >9) and one sample failed during library construction. The remaining 19 samples were prepared, sequenced, processed and analysed as previously described.²⁵ Differential expression of > 16,000 genes was analysed with edgeR (version 3.26.8). In brief, gene-wise expression in all proband sets (n = 10) was compared to expression in all control sets (n = 9) using negative binomial generalized linear models (GLM) and quasi-likelihood F-test as testing procedure. Gene expression changes were expressed as log2-fold changes with expression in the control group used as a baseline. Differentially expressed genes with an adjusted p-value (FDR) of less than 0.01 and an absolute log2-fold change of at least 1 were reported.

NanoLC-MS/MS analysis and data processing

Protein samples for nanoLC-MS/MS were generated from five fibroblast cell lines in biological duplicates (F1-IV.1, F1-IV.3, F2-III.3, F2-IV.1, F3-II.1) and compared to five control fibroblast cell lines (age and gender matched) in biological duplicates (Table S7). Nano LC MS/MS analysis and data processing was performed as previously described.²⁵

RESULTS

Gene burden analysis identifies an excess of heterozygous LoFs in families with spasticity or ataxia.

To detect enrichment for predicted pathogenic variants in novel genes for ataxia and spastic paraplegia, gene burden analysis was performed independently within a German cohort by a research group in Tuebingen (Germany) and within the 100KGP by researchers in London (U.K.), on a total of 3,169 patients and 33,141 controls across all cohorts.

For the German cohort, gene-based collapsing analysis (in 1,547 cases and 3,624 controls) revealed an exome-wide significant enrichment of rare variants only in *SPAST* (Table S1). Furthermore, the burden analysis indicated an enrichment of rare variants in *KIF5A*, *UCHL1*, and *POLR3A*, which, however, did not reach exome-wide significance (Table S1). While *SPAST* and *KIF5A*, which were top-listed in the burden analysis, are dominant-acting genes, *UCHL1* and *POLR3A*, have been associated with autosomal recessive disorders.^{26, 27} Surprisingly, the variants that generated the *UCHL1* signal were LoFs and did not derive from possible recessive *UCHL1* cases. A subsequent *UCHL1* enrichment analysis in the full in-house database containing 14,303 datasets (2,066 cases with HSP and/or HA, and 12,237 controls) revealed a significant enrichment of LoFs in cases. This enrichment reached exome-wide significance when compared to gnomAD controls (Table S2). The enrichment was more significant among individuals with both HSP and HA ($p = 6.536 \times 10^{-8}$, 3/272 cases vs. 3/182,146 gnomAD controls) than in the overall group with individuals with HSP and/or HA ($p = 5.375 \times 10^{-7}$, 4/2,066 cases vs. 3/182,146 gnomAD controls). Notably, the observed/expected (o/e) number of LoFs in gnomAD was 0, indicating a high intolerance of *UCHL1* for haploinsufficiency. Rare missense variants in *UCHL1* (MAF < 0.1%) from our total in-house database were not enriched in cases (Table S3).

UCHL1 had been also investigated as candidate gene for the clinical indication HA within the follow-up of the cohort-wise gene burden analysis in the rare disease component of the 100KGP (57,002 genomes sequenced from 27,591 families affected by rare diseases).¹⁶

The new gene burden analysis within the latest available 100KGP dataset of 35,422 rare disease families, including 1,103 HA probands used as cases and 20,904 non-neurological probands used as controls, revealed a statistically significant burden of either LoFs ($p = 1.5 \times 10^{-5}$, $q = 0.0231$, 5/1,103 cases vs. 3/20,904 controls, Table S2) or any variants highly predicted to be pathogenic (including LoFs), i.e. Exomiser variant score ≥ 0.80 , ($p = 2.0 \times 10^{-5}$, $q = 0.0265$, 6/1,103 cases vs. 7/20,904 controls) in *UCHL1*.

Figures 1, 2 and table S5 summarise the *UCHL1* variants and clinical phenotype.

The four different heterozygous LoF variants in *UCHL1* identified through gene burden analysis within the German cohort were from four independent, so far genetically unsolved families (Families 1-4, Figure 1a). Briefly, in family F1, the index proband F1-III.3 carried the frameshift variant c.64dup, p.(Val22glyfs*39) in *UCHL1*. Subsequently four affected and one healthy family member were recruited from this large autosomal dominant family and segregation of c.64dup, p.(Val22glyfs*39) was observed for all of them either via Sanger sequencing or via ES (Figure 1a). F1-IV.3 was submitted independently for diagnostic ES. Prior to ES, common repeat disorders causing late onset cerebellar ataxia (SCA 1,2,3,6,7,17) and CNVs in *SPAST* had been excluded. Having identified the same LoF variant in F1-IV.3, we were able to reconstruct the relationship to F1 by extending the family history (Figure 1a). Another frameshift variant, c.349_364del, p.(Phe117Argfs*33), was identified in individual F2-III.2. Three healthy sisters (F2-III.1, F2-III.6 and F2-III.7) and two affected brothers (F2-III.5 and F2-III.8) were available for segregation analyses (Figure 1a). One of her affected brother (F2-III.5) had an additional diagnosis of ALS and carried a heterozygous pathogenic *SOD1* variant, c.272A>C, p.(Asp91Ala). No other disease-causing or likely disease-causing variants in established genes related to HSPs, HAs or neuropathy could be detected in the ES of individual F2-III.2 and her brother F2-III.5. The daughter (F2-IV.1) of the remaining affected sister (F2-III.3) was subsequently diagnosed with ataxia and the same variant was identified independently by diagnostic GS. Finally, the other two individuals identified through the burden analysis, F3-II.1 and F4-II.1, were harboring a heterozygous c.385_388dup, p.(Ala130Glu fs*6)

variant and a splice variant c.527-1G>A, p.(?) respectively. In F3-II.1 a *de novo* status of the variant was confirmed by subsequent Sanger sequencing in unaffected parents and the healthy sister of F3-II.2 did not carry the variant (Figure 1a). Family members of F4-II.I were not available for segregation analysis.

Furthermore, three additional *UCHL1* families (F5, F6 and F7) were identified through international collaborators as following. One family (F5) carrying a c.387_388delAG, p.(Arg129Serfs*5) was identified through the RD-Connect Genome-Phenome Platform (<https://platform.rd-connect.eu/>) and two families (F6 and F7) were collected by communication with collaborators. Two affected sisters and the affected father from Family 6 (F6-III.1, F6-III.3 and F6-II.1) segregated for a LoF variant c.73C>T, p.(Gln25*). The same variant was found in a different unrelated neurological patient via diagnostic GS (F7) (Table S5).

In the U.K. cohort, 10 autosomal dominant families carrying either a LoF variant (n = 7) or a variant highly predicted to be pathogenic (n = 3) were altogether identified for *UCHL1*. First, five HA families with LoFs were identified, including F8, a male proband with an autosomal dominant family history of ataxia carrying the c.381-384del, p.(Asp128Glu fs*26) variant; F9, a duo with affected father and son both carrying the c.532C>T, p.(Arg178*) variant; F10, a singleton carrying the c.631G>T, p.(Glu211*) variant; F11, a singleton carrying the c.258insGG, p.(Asn88Gly fs*28); F12, a duo with affected mother and daughter both carrying the c.94insTGGG, p.(Leu34Gly fs*28) variant, and an autosomal dominant family history of disorder. The phenotypic data recorded on these families was suggestive of a late onset spastic ataxia with visual involvement, and this prompted the search for additional families in the 100KGP cohort with LoFs in *UCHL1*. Additional families were identified as detailed below. F13, a duo family with father and son with a dominant family history, recruited as HSP were identified as carrying the same variant found in family F9, c.532C>T, p.(Arg178*). In F14, a proband recruited under inherited optic neuropathy, was found to carry the c.116_117del, p.(Leu39Arg fs*21), also present in the mother, recorded as unaffected. The clinical re-examination of the family, revealed an autosomal dominant family history of ataxia, with the

mother and the maternal grandfather affected. Three more families (F15, F16, F17) were identified when assessing an excess in cases of variants highly predicted to be pathogenic, i.e. Exomiser variant score ≥ 0.80 . That first led to the identification of a proband with HA in family F15 carrying an in-frame duplication variant c.154_156dup, p.(Leu52dup); the same variant was also found in the proband from family F16 recruited under HSP and in another proband, and his sister recruited under HA and inherited optic neuropathy (F17) (Table S5). The c.154_156dup, p.(Leu52dup) variant present in those three families is absent in Gnomad and in the 100KGP dataset.

Clinical phenotypes

Detailed clinical information was available in 30 of 33 individuals from 17 families carrying 12 LoFs and a highly predicted pathogenic in-frame duplication in *UCHL1*. On clinical examination (Table S5), lower limb spasticity with elevated reflexes was present in 23 of 30 individuals. Gait ataxia was present in 27 individuals and 25 of them had predominantly cerebellar ataxia with either saccadic eye movements (16/30), dysarthria or dysphagia (8/30), or intention tremor (17/30). Two individuals presented with predominantly sensory ataxia. Reduced surface sensibility or pallesthesia in the lower limbs was present in 24 individuals, and sensory or sensorimotor axonal neuropathy could be demonstrated electrophysiologically in 11 of 20 examined patients. Eleven patients reported visual impairment, and optic atrophy was detected in 10 of 17 examined individuals. Disease onset varied from childhood to age 70 (median 49) with slow progression of the movement disorder according to medical history. In summary, the core phenotype consists of sensory or cerebellar ataxia (25/30), spastic paraplegia (23/30), sensory or sensorimotor neuropathy (11/20) and optic atrophy (10/17) (Figure 2, Table S5).

Some individuals differed from this core phenotype. F1-III.4 suffered from a generalized dystonia from the age of 53 years onwards and had developed, possibly independent from the dystonia symptom, a spastic-ataxic gait disorder at the age of 70 similar to the other family members. F2-III.5 presented lower motoneuron signs in addition to a spastic-ataxic phenotype,

clinically compatible with a slowly progressive amyotrophic lateral sclerosis. The most probable explanation is an additional identified likely pathogenic heterozygous *SOD1* variant (c.272A>C, [p.Asp91Ala]) explaining the overlapping features of ALS in F2-III.5.^{28,29} The most severely affected individual was F3-II.1. He had a history of childhood-onset developmental delay, followed by optic atrophy with severe visual impairment (visus c.c. 0.06 on both eyes) diagnosed around the age of 12 years. Spastic-ataxic gait disorder developed at the age of 25 years.

One individual (F12-III.2) also presented with early-onset visual difficulties (at 7 years) and was diagnosed with optic atrophy in his twenties. He is currently 24 years old and does not present signs of spasticity or ataxia, unlike his mother (F12-II.1).

Exploring dysregulated pathways in proband-derived fibroblasts

We next performed RNA-seq and nanoLC-MS/MS comparing five proband-derived fibroblast cell lines (F1-IV.1, F1-IV.3, F2-III.3, F2-IV.1, F3-II.1) with five age and gender matched control cell lines. From the RNA-seq data, 174 genes were significantly up- or downregulated (false discovery rate (FDR) < 0.01 and absolute |log FC| ≥ 0.5, Table S6). In the NanoLC-MS/MS data, 75 proteins were significantly up- or downregulated (log Student's T-test p-value ≤ 0.05 and absolute |log FC| ≥ 0.5, Table S7). Significant changes in mRNA levels (FDR < 0.01) correlated well with significant changes in protein levels, detected by MS (rho = 0.85, $p = 2.2 \times 10^{-16}$) (Figure S1), implicating reliability of these data.

Overall *UCHL1* transcript expression levels were not significantly different between patients and controls (Figure 3a). However, the LoFs (p.Val22GlyTerfs39, p.Phe117ArgfsTer33 and p.Ala130GlufsTer6) were covered in the RNA-seq data of the respective patients with an allele frequency of only 0.04±0.03, indicating nonsense-mediated decay (Figure 3b). Accordingly, protein levels of UCHL1 were significantly decreased (-2.4 logFC, Figure 3c). Remarkably, this unbiased approach even showed UCHL1 as the protein with the largest decrease in protein level (Figure 3c). An interaction network based on the 30 most up- or downregulated proteins was computed using string-db (<https://string-db.org/>),

revealing a significant enrichment of interactions among these proteins (protein-protein interaction enrichment $p = 1.17e-7$, Figure S2). Of note, the protein with the highest increase in protein level (2.05 logFC) was MME (membrane metallo-endopeptidase or neprilysin) which was directly linked to UCHL1 (Figure S2). MME cleaves and inactivates several peptides and is known to degrade amyloid-beta (A β). Furthermore, autosomal recessive and dominant-acting variants in *MME* have been implicated in the pathogenesis of Charcot-Marie-Tooth disease type 2T and spinocerebellar ataxia type 43.³⁰⁻³² Both MME and UCHL1 are connected with the metabolism of amyloid- β precursor protein (APP) and the clearance of A β . UCHL1 has been well described to inactivate the Beta-Secretase 1 (BACE1), the major beta-secretase for the generation of A β peptides from APP.³³ By including APP additionally to the 30 most up- or downregulated proteins in the network analysis, it seems that APP acts as a central connecting node in the interaction network of dysregulated proteins (Figure 3d).

DISCUSSION

In this study, we provide several lines of evidence that heterozygous LoFs in *UCHL1* are the genetic cause of an autosomal dominant inherited neurodegenerative disorder with a distinct phenotype. Two independent case-control burden analyses prioritized *UCHL1* among the top hits. Surprisingly the signal was not generated by previously described missense variants that were associated with autosomal recessive SPG79⁶⁻⁸, but mostly due to heterozygous LoFs.

In total, 12 different heterozygous *UCHL1* LoFs were identified in 28 patients from 16 families showing a clear autosomal dominant inheritance and a common core phenotype. This core phenotype consists of a movement disorder with spastic paraplegia, ataxia, and often sensorimotor neuropathy. Visual impairment and optic atrophy were other frequent features. While some probands had early-onset visual impairment, others only had subclinical optic atrophy or no optic atrophy at all. During extended screening for *UCHL1* variants, we also identified three independent families with the heterozygous duplication c.154_156dup, p.(Leu52dup). Probands from all three families (F13, F14, F16.II-2, F16.III-1) presented with

the specific combination of optic atrophy and late-onset spastic-ataxia. Therefore, we consider it likely that these variants are also pathogenic.

Previously, bi-allelic variants in *UCHL1* have been associated with the autosomal recessive inherited SPG79. To date, four SPG79 families with ten affected subjects have been reported. In 2013, Bilguvar et al. described a consanguineous family of Turkish origin with three affected siblings who harbored a homozygous missense variant (c.20A>C, [p.Glu7Ala]) and presented an early-onset progressive neurodegenerative syndrome with visual loss, ataxia, spasticity, and cognitive impairment.⁶ *Uchl1* knockout mice displayed spastic gait movements and progressive paralyses in their hind limbs consistent with the spastic-ataxia phenotype of the SPG79 family.³⁴ Subsequently, compound heterozygous missense variants (c.533G>A, p.[Arg178Gln] and c.647C>A, [p.Ala216Asp]) were cosegregated in a Norwegian family of three affected siblings and a homozygous splice variant (c.459+2T>C, p.[?]) was identified in an Indian family with two affected siblings, both families demonstrating a phenotype similar to the previously reported SPG79 family.^{7, 8} The splice variant was inherited from unaffected consanguineous parents. This homozygous splice variant (c.459+2T>A, p.[?]) affects the donor splice-site of exon 6, possibly leading to a skipping of exon 6, which would create an in-frame deletion of 16 amino acids.⁷ In contrast, the splice variant identified in individual F5-II.1 is located in the acceptor splice site of intron 7, is predicted to induce skipping of exon 8. We were not able to obtain fibroblasts from this patient to confirm a splicing defect and haploinsufficiency, but it is very likely that a deletion of exon 8 would lead to a frameshift and premature truncation possibly inducing NMD similar to the other identified LoFs. Another smaller homozygous in-frame deletion c.627_629del, p.(Gly210del) has been reported in two siblings, showing childhood-onset visual impairment, progressive spasticity, and ataxia, compatible with the diagnosis of Behr syndrome.³⁵ Thus, identical neurological systems are affected in both the previously reported recessive SPG79 and the currently reported cohort with heterozygous LoFs, while the currently reported probands have a milder course with a later disease onset on average.

By exploring transcriptomics and proteomics data of patient-derived fibroblasts, we have strengthened the hypothesis that haploinsufficiency of *UCHL1* is the likely pathomechanism. The RNA-seq data indicated NMD and more importantly, the mass spectrometry-based proteomics data showed significantly decreased *UCHL1* levels. Regarding other dysregulated proteins, our analysis pattern suggests a link to Amyloid- β degradation pathways, and the overexpression of *MME* could be in part a compensatory mechanism. Of note, pathogenic variants in *MME* have been associated with autosomal dominant SCA43 with neuropathy.³² The role of *UCHL1* in protein degradation pathways and the ubiquitin-proteasome systems has been suggested as the mechanism for the involvement of *UCHL1* in the pathogenesis of several neurodegenerative disorders. In detail, two missense variants in *UCHL1* have been implicated in PD. While the change p.Ile93Met was described to cause early-onset PD with an incomplete penetrance exhibiting a reduced hydrolase activity of approximately 50%, the polymorphism p.Ser18Tyr appeared to be a protective factor for PD that showed an increased hydrolase activity of 112.6%.^{15, 36-38} However, both theories have also been negated by several subsequent meta analyses studies.³⁹⁻⁴¹ Some data have also shown that *UCHL1* might be involved in the pathophysiology and disease progression of AD and ALS. Reduced *UCHL1* expression was observed in individuals with AD and overexpression of *UCHL1* improved beta-amyloid-induced synaptic dysfunction and memory deficits in AD mouse models^{13, 42, 43} Furthermore, quantitative proteomic studies revealed elevated *UCHL1* protein levels in cerebrospinal fluid of individuals with ALS suggesting *UCHL1* as a potential biomarker that might be involved in the disease progression of ALS.^{44, 45}

In case of the recessive SPG79, functional data so far suggested different pathomechanisms. The change p.Glu7Ala causing SPG79 showed reduced enzymatic hydrolase activity of <10%, therefore, loss-of-function was the initially suggested disease-causing pathomechanism for the recessive disorder.⁶ However, the two missense variants that were in a compound heterozygous state in three affected SPG79 individuals had two opposing pathomechanisms. While p.Ala216Asp proteins were degraded, the p.Arg178Gln had enhanced enzymatic activity. Of note, the p.Ala216Asp mRNA was not degraded, indicating

that NMD was not the cause for the absent detection of p.Ala216Asp proteins.⁸ The consequences of the homozygous splice variant c.459+2T>A and the in-frame deletion p.Gly210del has not been explored yet.^{7, 35} Since the parents were reportedly asymptomatic, it is possible that the produced UCHL1 proteins either exert a different so far unknown function leading to the recessive disorder or sufficient residual function to escape the autosomal dominant phenotype in a heterozygous state.

Overall, these studies support the evidence that UCHL1 is involved in neurodegeneration, however the exact pathomechanism of its variants for recessive disorders and other common neurodegenerative disorders such as PD and AD remains unclear. Notably, natural and synthetic antisense to mouse *Uchl1* (AS-*Uchl1*) have shown to activate *UCHL1* mRNA translation increasing protein synthesis at post-translational level *in vitro*.⁴⁶ On the basis of this discovery, the use of AS *Uchl1*-derived long non-coding RNAs, named SINEUPs, has been proposed as potential new RNA-based therapy for gene-specific haploinsufficiency diseases.⁴⁷ In this regard, patients harboring LoFs in *UCHL1* and possibly other *UCHL1*-associated disorders could potentially be managed in the future using the already discovered AS-*Uchl1* as agent.

Our statistic analyses, supporting segregation data as well as functional evaluation provide evidence of *UCHL1* haploinsufficiency as the pathomechanism underlying an autosomal dominant neurological disorder presenting with spastic paraplegia, ataxia, polyneuropathy, and often optic atrophy. The disease presentation is similar, but overall milder than the previously reported recessive disorder SPG79. Our proteomics analysis has further strengthened the role of UCHL1 in protein degradation pathways, especially related to APP. These degradation pathways might be one of the reasons for the above-mentioned involvement in the pathogenesis of several different neurodegenerative disorders. Continuous exploration of UCHL1 function in various neurodegenerative diseases and of mechanisms by which single heterozygous or homozygous variants lead to specific phenotypes may provide further insight into the pathogenesis of neurodegenerative diseases.

518
519
520
521
522
523
524
525
526
527
528
529
530
531
532
533
534
535
536
537
538
539
540
541
542
543
544
545

SUPPLEMENTAL DATA

Figure S1: Correlation of RNA-Seq and NanoLC-MS/MS data

Figure S2: Interactome based on most over-or underexpressed proteins

Table S1: Gene-based rare-variant burden analysis results using 1,547 diagnostic cases with either spastic paraplegia, ataxia or both phenotypes and 3,624 controls.

Table S2: Count of different *UCHL1* LoFs alleles in the transcript NM_004181.4/ENST00000284440.4 in the German and U.K. cohorts, and in gnomAD browser (v2.1.1 and v3.1.1, non-neuro).

Table S3: Count of different *UCHL1* missense variants (NM_004181.4/ENST00000284440.4) with MAF < 0.1% in gnomAD in the German and U.K. cohorts, and in gnomAD browser (v2.1.1 and v3.1.1, non-neuro).

Table S4: Gene variant position and population frequency of *UCHL1* (NM_004181.4/ENST00000284440.4) LoFs identified in different families

Table S5: Clinical features of patients with heterozygous LoFs in *UCHL1*

Table S6: Expression levels from RNA-seq based on fibroblasts from F1-IV.1, F1-IV.3, F2-III.2, F2-IV.1, F3-II.1 in comparison to age and gender matched controls

Table S7: Results from nanoLC-MS/MS based on fibroblasts from F1-IV.1, F1-IV.3, F2-III.2, F2-IV.1, F3-II.1 in comparison to controls

546

547 **DECLARATION OF INTERESTs**

548 The authors declare no competing interests.

549

550 **ACKNOWLEDGEMENTS**

551 We thank all the families for their participation. LS, MS, OR and HH are members of the
552 European Reference Network for Rare Neurological Diseases (ERN-RND). TBH was
553 supported by the Deutsche Forschungsgemeinschaft (DFG, German Research Foundation:
554 418081722, 433158657). HH was supported by the intramural fortune program (#2554-0-0)
555 and by the DFG under the project number HE 8803/1–1. GKT is supported by an MRC Senior
556 Clinical Fellowship (MR/V007068/1).

557

558 **CONSORTIA**

559 **Members of The Genomics England Research Consortium:**

560 J. C. Ambrose¹, P. Arumugam¹, E. L. Baple¹, M. Bleda¹, F. Boardman-Pretty^{1,2}, J. M. Boissiere¹,
561 C. R. Boustred¹, H. Brittain¹, M. J. Caulfield^{1,2}, G. C. Chan¹, C. E. H. Craig¹, L. C. Daugherty¹,
562 A. de Burca¹, A. Devereau¹, G. Elgar^{1,2}, R. E. Foulger¹, T. Fowler¹, P. Furió-Tarí¹, J. M. Hackett¹,
563 D. Halai¹, A. Hamblin¹, S. Henderson^{1,2}, J. E. Holman¹, T. J. P. Hubbard¹, K. Ibáñez^{1, 2}, R.
564 Jackson¹, L. J. Jones^{1,2}, D. Kasperaviciute^{1,2}, M. Kayikci¹, L. Lahnstein¹, K. Lawson¹, S. E. A.
565 Leigh¹, I. U. S. Leong¹, F. J. Lopez¹, F. Maleady-Crowe¹, J. Mason¹, E. M. McDonagh^{1,2}, L.
566 Moutsianas^{1,2}, M. Mueller^{1,2}, N. Murugaesu¹, A. C. Need^{1,2}, C. A. Odhams¹, C. Patch^{1,2}, D.
567 Perez-Gil¹, D. Polychronopoulos¹, J. Pullinger¹, T. Rahim¹, A. Rendon¹, P. Riesgo-Ferreiro¹, T.
568 Rogers¹, M. Ryten¹, K. Savage¹, K. Sawant¹, R. H. Scott¹, A. Siddiq¹, A. Sieghart¹, D.
569 Smedley^{1,2}, K. R. Smith^{1,2}, A. Sosinsky^{1,2}, W. Spooner¹, H. E. Stevens¹, A. Stuckey¹, R.
570 Sultana¹, E. R. A. Thomas^{1,2}, S. R. Thompson¹, C. Tregidgo¹, A. Tucci^{1,2}, E. Walsh¹, S. A.
571 Watters¹, M. J. Welland¹, E. Williams¹, K. Witkowska^{1,2}, S. M. Wood^{1,2}, M. Zarowiecki¹

572 ¹Genomics England, London, UK

573 ²William Harvey Research Institute, Queen Mary University of London, London, EC1M 6BQ,
574 UK

575

576 **WEB RESOURCES**

577 The URLs for the data presented herein are as follows:

578 gnomAD server, <https://gnomad.broadinstitute.org/>

579 GTEx Portal, <https://gtexportal.org>

Online Mendelian Inheritance in Man (OMIM), <https://omim.org/>
megSAP pipeline, <https://github.com/imgag/megSAP>
string-db (<https://string-db.org/>)
RD-Connect Genome-Phenome Platform, <https://platform.rd-connect.eu/>

DATA AND CODE AVAILABILITY

Additional data from this study can be provided upon reasonable request

REFERENCES

1. Bourassa CV, Meijer IA, Merner ND, et al. VAMP1 mutation causes dominant hereditary spastic ataxia in Newfoundland families. *Am J Hum Genet.* 2012 Sep 7;91(3):548-52.
2. de Bot ST, Willemsen MA, Vermeer S, Kremer HP, van de Warrenburg BP. Reviewing the genetic causes of spastic-ataxias. *Neurology.* 2012 Oct 2;79(14):1507-14.
3. Meijer IA, Hand CK, Grewal KK, Stefanelli MG, Ives EJ, Rouleau GA. A locus for autosomal dominant hereditary spastic ataxia, SAX1, maps to chromosome 12p13. *Am J Hum Genet.* 2002 Mar;70(3):763-9.
4. Synofzik M, Schule R. Overcoming the divide between ataxias and spastic paraplegias: Shared phenotypes, genes, and pathways. *Movement disorders : official journal of the Movement Disorder Society.* 2017 Mar;32(3):332-45.
5. Ngo KJ, Rexach JE, Lee H, et al. A diagnostic ceiling for exome sequencing in cerebellar ataxia and related neurological disorders. *Human mutation.* 2020 Feb;41(2):487-501.
6. Bilguvar K, Tyagi NK, Ozkara C, et al. Recessive loss of function of the neuronal ubiquitin hydrolase UCHL1 leads to early-onset progressive neurodegeneration. *Proc Natl Acad Sci U S A.* 2013 Feb 26;110(9):3489-94.
7. Das Bhowmik A, Patil SJ, Deshpande DV, Bhat V, Dalal A. Novel splice-site variant of UCHL1 in an Indian family with autosomal recessive spastic paraplegia-79. *J Hum Genet.* 2018 Aug;63(8):927-33.
8. Rydning SL, Backe PH, Sousa MML, et al. Novel UCHL1 mutations reveal new insights into ubiquitin processing. *Hum Mol Genet.* 2017 Mar 15;26(6):1031-40.
9. Lowe J, McDermott H, Landon M, Mayer RJ, Wilkinson KD. Ubiquitin carboxyl-terminal hydrolase (PGP 9.5) is selectively present in ubiquitinated inclusion bodies characteristic of human neurodegenerative diseases. *J Pathol.* 1990 Jun;161(2):153-60.
10. Wilkinson KD, Lee KM, Deshpande S, Duerksen-Hughes P, Boss JM, Pohl J. The neuron-specific protein PGP 9.5 is a ubiquitin carboxyl-terminal hydrolase. *Science.* 1989 Nov 3;246(4930):670-3.
11. Komander D, Clague MJ, Urbe S. Breaking the chains: structure and function of the deubiquitinases. *Nat Rev Mol Cell Biol.* 2009 Aug;10(8):550-63.
12. Jara JH, Frank DD, Ozdinler PH. Could dysregulation of UPS be a common underlying mechanism for cancer and neurodegeneration? Lessons from UCHL1. *Cell Biochem Biophys.* 2013 Sep;67(1):45-53.
13. Choi J, Levey AI, Weintraub ST, et al. Oxidative modifications and down-regulation of ubiquitin carboxyl-terminal hydrolase L1 associated with idiopathic Parkinson's and Alzheimer's diseases. *J Biol Chem.* 2004 Mar 26;279(13):13256-64.

14. Konya C, Hatanaka Y, Fujiwara Y, et al. Parkinson's disease-associated mutations in alpha-synuclein and UCH-L1 inhibit the unconventional secretion of UCH-L1. *Neurochem Int.* 2011 Aug;59(2):251-8.
15. Nishikawa K, Li H, Kawamura R, et al. Alterations of structure and hydrolase activity of parkinsonism-associated human ubiquitin carboxyl-terminal hydrolase L1 variants. *Biochem Biophys Res Commun.* 2003 Apr 25;304(1):176-83.
16. Investigators GPP, Smedley D, Smith KR, et al. 100,000 Genomes Pilot on Rare-Disease Diagnosis in Health Care - Preliminary Report. *N Engl J Med.* 2021 Nov 11;385(20):1868-80.
17. Falb RJ, Muller AJ, Klein W, et al. Bi-allelic loss-of-function variants in KIF21A cause severe fetal akinesia with arthrogryposis multiplex. *J Med Genet.* 2021 Nov 5.
18. Weisschuh N, Mazzola P, Heinrich T, et al. First submicroscopic inversion of the OPA1 gene identified in dominant optic atrophy - a case report. *BMC Med Genet.* 2020 Nov 26;21(1):236.
19. Richards S, Aziz N, Bale S, et al. Standards and guidelines for the interpretation of sequence variants: a joint consensus recommendation of the American College of Medical Genetics and Genomics and the Association for Molecular Pathology. *Genet Med.* 2015 May;17(5):405-24.
20. Susak H, Serra-Saurina L, Demidov G, et al. Efficient and flexible Integration of variant characteristics in rare variant association studies using integrated nested Laplace approximation. *PLoS Comput Biol.* 2021 Feb;17(2):e1007784.
21. Smedley D, Jacobsen JO, Jager M, et al. Next-generation diagnostics and disease-gene discovery with the Exomiser. *Nat Protoc.* 2015 Dec;10(12):2004-15.
22. Martin AR, Williams E, Foulger RE, et al. PanelApp crowdsources expert knowledge to establish consensus diagnostic gene panels. *Nat Genet.* 2019 Nov;51(11):1560-5.
23. Dolzhenko E, Deshpande V, Schlesinger F, et al. ExpansionHunter: a sequence-graph-based tool to analyze variation in short tandem repeat regions. *Bioinformatics.* 2019 Nov 1;35(22):4754-6.
24. Kohler S, Gargano M, Matentzoglou N, et al. The Human Phenotype Ontology in 2021. *Nucleic Acids Res.* 2021 Jan 8;49(D1):D1207-D17.
25. Hengel H, Hannan SB, Dyack S, et al. Bi-allelic loss-of-function variants in BCAS3 cause a syndromic neurodevelopmental disorder. *Am J Hum Genet.* 2021 Jun 3;108(6):1069-82.
26. Parodi L, Fenu S, Barbier M, et al. Spastic paraplegia due to SPAST mutations is modified by the underlying mutation and sex. *Brain.* 2018 Dec 1;141(12):3331-42.
27. Goizet C, Boukhris A, Mundwiller E, et al. Complicated forms of autosomal dominant hereditary spastic paraplegia are frequent in SPG10. *Human mutation.* 2009 Feb;30(2):E376-85.
28. Andersen PM, Nilsson P, Ala-Hurula V, et al. Amyotrophic lateral sclerosis associated with homozygosity for an Asp90Ala mutation in CuZn-superoxide dismutase. *Nature Genetics.* 1995 1995/05/01;10(1):61-6.
29. Turner MR, Rabiner EA, Al-Chalabi A, et al. Cortical 5-HT1A receptor binding in patients with homozygous D90A SOD1 vs sporadic ALS. *Neurology.* 2007 Apr 10;68(15):1233-5.
30. Auer-Grumbach M, Toegel S, Schabhüttl M, et al. Rare Variants in MME, Encoding Metalloprotease Neprilysin, Are Linked to Late-Onset Autosomal-Dominant Axonal Polyneuropathies. *Am J Hum Genet.* 2016 Sep 1;99(3):607-23.
31. Higuchi Y, Hashiguchi A, Yuan J, et al. Mutations in MME cause an autosomal-recessive Charcot-Marie-Tooth disease type 2. *Ann Neurol.* 2016 Apr;79(4):659-72.
32. Depondt C, Donatello S, Rai M, et al. MME mutation in dominant spinocerebellar ataxia with neuropathy (SCA43). *Neurol Genet.* 2016 Oct;2(5):e94.
33. Guglielmotto M, Monteleone D, Vasciaveo V, et al. The Decrease of Uch-L1 Activity Is a Common Mechanism Responsible for Aβ 42 Accumulation in Alzheimer's and Vascular Disease. *Front Aging Neurosci.* 2017;9:320.
34. Chen F, Sugiura Y, Myers KG, Liu Y, Lin W. Ubiquitin carboxyl-terminal hydrolase L1 is required for maintaining the structure and function of the neuromuscular junction. *Proc Natl Acad Sci U S A.* 2010 Jan 26;107(4):1636-41.
35. McMacken G, Lochmuller H, Bansagi B, et al. Behr syndrome and hypertrophic cardiomyopathy in a family with a novel UCHL1 deletion. *J Neurol.* 2020 Dec;267(12):3643-9.

36. Leroy E, Boyer R, Auburger G, et al. The ubiquitin pathway in Parkinson's disease. *Nature*. 1998 Oct 1;395(6701):451-2.
37. Maraganore DM, Lesnick TG, Elbaz A, et al. UCHL1 is a Parkinson's disease susceptibility gene. *Ann Neurol*. 2004 Apr;55(4):512-21.
38. Tan EK, Puong KY, Fook-Chong S, et al. Case-control study of UCHL1 S18Y variant in Parkinson's disease. *Movement disorders : official journal of the Movement Disorder Society*. 2006 Oct;21(10):1765-8.
39. Healy DG, Abou-Sleiman PM, Wood NW. Genetic causes of Parkinson's disease: UCHL-1. *Cell Tissue Res*. 2004 Oct;318(1):189-94.
40. Mellick GD, Silburn PA. The ubiquitin carboxy-terminal hydrolase-L1 gene S18Y polymorphism does not confer protection against idiopathic Parkinson's disease. *Neurosci Lett*. 2000 Oct 27;293(2):127-30.
41. Healy DG, Abou-Sleiman PM, Casas JP, et al. UCHL-1 is not a Parkinson's disease susceptibility gene. *Ann Neurol*. 2006 Apr;59(4):627-33.
42. Zhang M, Cai F, Zhang S, Zhang S, Song W. Overexpression of ubiquitin carboxyl-terminal hydrolase L1 (UCHL1) delays Alzheimer's progression in vivo. *Sci Rep*. 2014 Dec 3;4:7298.
43. Gong B, Cao Z, Zheng P, et al. Ubiquitin hydrolase Uch-L1 rescues beta-amyloid-induced decreases in synaptic function and contextual memory. *Cell*. 2006 Aug 25;126(4):775-88.
44. Oeckl P, Weydt P, Thal DR, Weishaupt JH, Ludolph AC, Otto M. Proteomics in cerebrospinal fluid and spinal cord suggests UCHL1, MAP2 and GPNMB as biomarkers and underpins importance of transcriptional pathways in amyotrophic lateral sclerosis. *Acta Neuropathol*. 2020 Jan;139(1):119-34.
45. Zhu S, Wuolikainen A, Wu J, et al. Targeted Multiple Reaction Monitoring Analysis of CSF Identifies UCHL1 and GPNMB as Candidate Biomarkers for ALS. *J Mol Neurosci*. 2019 Dec;69(4):643-57.
46. Carrieri C, Cimatti L, Biagioli M, et al. Long non-coding antisense RNA controls Uchl1 translation through an embedded SINEB2 repeat. *Nature*. 2012 Nov 15;491(7424):454-7.
47. Zucchelli S, Fasolo F, Russo R, et al. SINEUPs are modular antisense long non-coding RNAs that increase synthesis of target proteins in cells. *Front Cell Neurosci*. 2015;9:174.

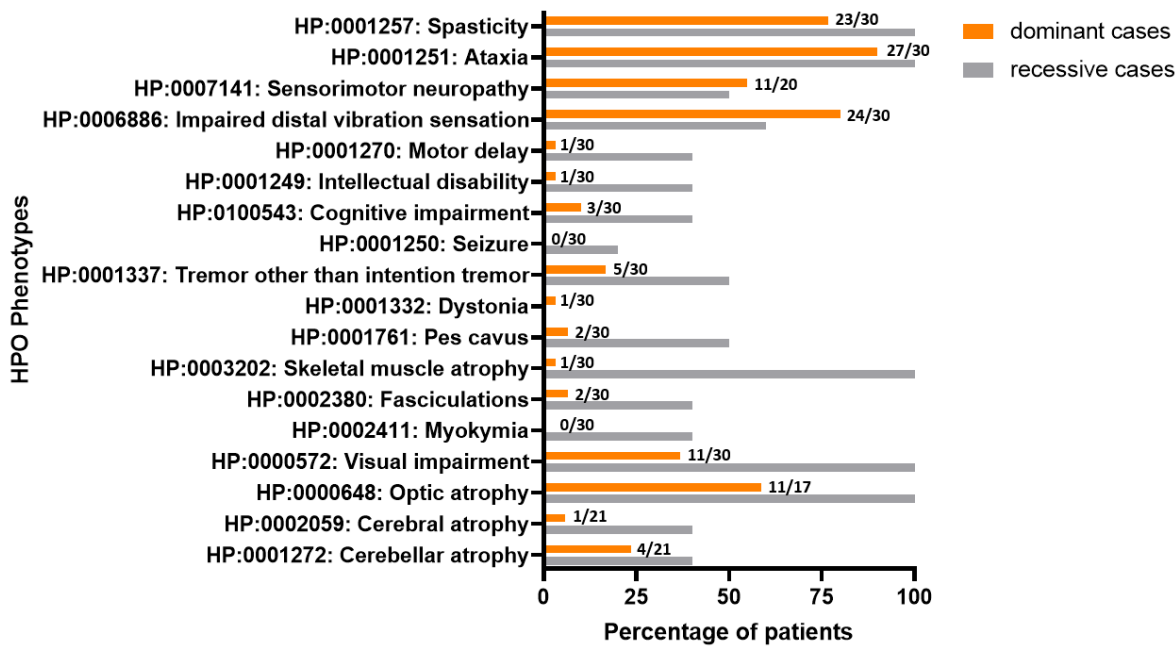
FIGURE TITLES AND LEGENDS

Figure 1: Pedigrees of six *UCHL1* Families, and Structure of *UCHL1*

(a) Pedigrees of families segregating heterozygous LoFs in *UCHL1* (F1-F14), and one *UCHL1* inframe duplication (F15-F17). Affected family members are shown in closed symbols and healthy family members with open symbols. Heterozygous variant carriers are presented with m/wt while non-carriers are marked with wt/wt. wt indicates for wildtype and m for mutation. Other family members were not available for genetic testing.

(b) Graphical illustration of *UCHL1* gene and protein domain structures, and position of the identified variants. Newly reported LoFs are written in red and previously published variants in black.

Figure 2: Distribution of symptoms in *UCHL1* patients



Bars represent the percentage of patients with heterozygous *UCHL1* variants (orange bars) and the autosomal recessive disorder, SPG79 (blue bars), presenting given symptoms. The symptoms are listed using the Human Phenotype Ontology (HPO) Terms.

Figure 3: Transcriptomics and proteomics data illustration

